

Dramatic impurity effects on the charge-density wave in potassium molybdenum bronze

L. F. Schneemeyer, F. J. DiSalvo, S. E. Spengler, and J. V. Waszczak

AT&T Bell Laboratories, Murray Hill, New Jersey 07974

(Received 5 March 1984; revised manuscript received 20 June 1984)

Potassium molybdenum bronze, $K_{0.30}MoO_3$, undergoes a charge-density-wave (CDW-) driven phase transition at 180 K, below which nonlinear current-voltage characteristics are observed. Behavior is similar to that observed in $NbSe_3$ and is currently understood based on models which involve charge transport by the CDW. The effects of impurities on CDW phenomena has been a subject of considerable interest. Two types of substitutional doping are possible in the $K_{0.30}MoO_3$ structure. In the alloy system, $K_{0.30-x}Rb_xMoO_3$, disorder is introduced on the alkali sublattice while in the alloy system, $K_{0.30}Mo_{1-x}W_xO_3$, the isoelectronic element tungsten is substituted for molybdenum. We show that the effects of tungsten substitution are very large, larger than such doping effects in other CDW systems, whereas alkali substitution produces only small effects. The data obtained on the $K_{0.30}Mo_{1-x}W_xO_3$ system suggest that the low-temperature CDW coherence length becomes very short at low tungsten concentrations.

INTRODUCTION

The blue potassium molybdenum bronze, $K_{0.30}MoO_3$, undergoes a charge-density-wave- (CDW-) driven phase transition at 180 K.¹ In the CDW state, $K_{0.30}MoO_3$ shows a variety of nonlinear effects such as nonohmic current-voltage characteristics above a sharp threshold field.² Such nonlinear behavior has been associated with a moving CDW ("sliding CDW") in $NbSe_3$ and related transition-metal trichalcogenides³ and recently has been seen in transition-metal tetrachalcogenide halides such as $(TaSe_4)_2I$.⁴ Impurities play a major role in CDW transport. Ong *et al.* showed that the threshold field E_R increased with increasing impurity concentration^{5,6} in agreement with ideas of Lee and Rice on the pinning of a rigid CDW to impurities.⁷ Recently, it has been suggested that TaS_3 (Ref. 8) and $K_{0.30}MoO_3$ (Ref. 9) are commensurate at low temperature. The observation of a finite threshold field in TaS_3 and $K_{0.30}MoO_3$ at low temperature is then inconsistent with the pinning of a rigid CDW and suggests charge transport mediated by CDW discommensurations¹⁰ or dislocations.⁷ If so, impurity pinning would remain important even in the commensurate phase.

The effect of impurities on CDW phenomena has been the subject of considerable interest. Theoretical models that go beyond the mean-field description suggest that infinite long-range order cannot be established in CDW systems in the presence of impurities or defects.¹¹ There is, strictly speaking, no phase transition or temperature at which the derivatives of the free energy show discontinuous or singular behavior. Rather, local CDW distortions are induced about each impurity. These distortions have a moderate amplitude even above the phase-transition temperature of the pure material (T_0), but the distortions have a short range (short coherence length). The coherence length grows rapidly as the temperature is decreased in the vicinity of T_0 , but it saturates at some temperature below T_0 . The limiting value of the coherence length is determined by the strength of the impurity potential and

the impurity concentration. This expected finite CDW coherence has not yet been experimentally observed.¹² In sliding-CDW conductors such as $NbSe_3$, impurities or other disorders have been shown to result in increased threshold fields for the depinning of the CDW,^{5,6,12-15} but little is known about changes in other solid-state properties.

Two types of substitutional doping are possible in the $K_{0.30}MoO_3$ structure. By substituting rubidium for potassium, forming the alloy system $K_{0.30-x}Rb_xMoO_3$, disorder can be introduced on the alkali sublattice. $K_{0.30}MoO_3$ and $Rb_{0.30}MoO_3$ have isomorphous structures and nearly identical properties including sliding-CDW behavior, thus observed changes can be attributed to alkali disorder. Since the conduction band is based on a combination of Mo t_{2g} orbitals and oxygen $p\pi$ orbitals in the MoO_3 layer,¹⁶ the effects of alkali disorder are expected to be weak. Either isoelectronic or nonisoelectronic substituents can occupy the molybdenum site. Although some doped samples of $K_{0.30}MoO_3$ have been examined,¹⁷ no systematic studies have been reported. Tungsten, which is isoelectronic with molybdenum, can be substituted for molybdenum to form the alloy systems $K_{0.30}Mo_{1-x}W_xO_3$ ($x < 0.40$). The presence of the W impurity should have a strongly perturbing influence by directly disrupting the number of overlapping Mo d_{z^2} orbitals near the W-impurity site, producing large effects on the onset temperature and on the threshold field. In this study, we show that the effects of tungsten substitution are larger than those produced by doping of other CDW systems, whereas alkali substitution produces only small effects.

SAMPLE PREPARATION

Crystals were grown electrochemically as described elsewhere.¹⁸ 99.9% K_2MoO_4 , Rb_2MoO_4 , and MoO_3 (Cerac) were dried before use. The molybdenum-to-tungsten ratio in the melt controlled the tungsten concentration in the tungsten-doped samples. Fluorescence microprobe exam-

ination showed that the tungsten concentration was constant within a given batch of crystals and that the tungsten concentration in the crystals scaled with the tungsten concentration in the melt. Chemical analysis of selected samples (by Schwartzkopf Analytical Laboratories) showed that the tungsten concentration in the crystals was a factor of four greater than the tungsten concentration in the melt. The mass of crystals grown from each melt was a small fraction of the initial-melt mass to ensure compositional uniformity in the crystals. Alkali concentrations were controlled by the rubidium to potassium concentrations in the melt with concentrations in the crystals verified by atomic absorption analysis. Powder x-ray diffraction confirmed that the monoclinic $K_{0.30}MoO_3$ structure was maintained in all of the samples studied here.

MEASUREMENTS

Electrical resistivity measurements parallel to the monoclinic b axis were made in four-probe configurations on cleaved samples with ultrasonically soldered indium contacts. Rectangular samples were chosen. Current contacts covered the ends of the sample completely to ensure a uniform current distribution in the sample. Typically, ρ versus temperature was obtained by cooling from room temperature to 4.2 K at 1 K/min (slowed to about 0.5 K/min near the transition). Uncertainties in the absolute accuracy of the resistivity as large as 20% are due to uncertainties in measurements of sample size and to the finite size of the voltage contacts.

Magnetic susceptibility was measured on a number of samples from 4.2 to 300 K using the Faraday technique. Details of this apparatus are described elsewhere.¹⁹ The relative accuracy of χ_g is approximately $\pm 1 \times 10^{-10}$ emu/g or less depending on the sample size, but the absolute accuracy of the susceptibility relative to several standards is 2%. The susceptibility anisotropy of nominally pure $K_{0.30}MoO_3$ at room temperature as discussed in detail elsewhere,²⁰ is approximately a factor of 0.9 in the (201) cleavage plane and a factor of 2.5 perpendicular to these planes. However, the susceptibility anomaly is similar in shape and amplitude in all crystal orientations thus allowing reliable determination of relative changes in the susceptibility of doped samples. The samples consisted of a number of rectangular crystals whose b axes are parallel to the long crystal length. These crystals were held in a thin quartz tube so that the b axes of the crystals were close to perpendicular to the magnetic field. Since the sample tube was free to rotate, upon application of the magnetic field, the sample rotated to the maximum susceptibility direction perpendicular to the b axis. However, since some of the crystals were not perfectly aligned, we obtained values of the susceptibility in several samples of $K_{0.30}MoO_3$ that were up to 10–15% smaller than the largest principal value (0.114×10^{-6} emu/g at 300 K). All of the samples had the same room-temperature value independent of composition within the $\pm 7\%$ scatter that was expected due to this misorientation of the crystallites. There was no systematic trend in the variation of the room-temperature susceptibility with composition (within this 7% scatter). Since the changes in the susceptibility

induced by the CDW are much larger than this scatter, we chose to normalize all of the data to the same value of 0.114×10^{-6} emu/g at room temperature. Small Curie contributions to the susceptibility were subtracted out following usual procedures.¹⁹ Samples showed no evidence of ferromagnetic impurities.

RESULTS

Figure 1 shows the gram susceptibility as a function of temperature for a series of tungsten-substituted $K_{0.30}MoO_3$ samples. In nominally pure $K_{0.30}MoO_3$, the susceptibility is paramagnetic with a small temperature dependence from room temperature to about 200 K. Below this temperature the susceptibility drops steeply to diamagnetic behavior at low temperature. A small anomaly of unknown origin is noted near 40 K. At very low tungsten substitutional doping levels, < 2 mol % W, the anomaly near 180 K is observed to round and broaden. Well above or below 180 K, the susceptibility is identical with $K_{0.30}MoO_3$, including the presence of the small kink anomaly near 40 K. As the tungsten concentration is increased further, the anomaly continues to round and broaden and the size of the susceptibility drop below the transition decreases. Figure 2 shows the numerical derivative of the data obtained by least-squares fitting six data points at a time to $\chi = a + b \Delta T + c (\Delta T)^2$. The six data points generally span 3 or 4 K, and we plot the value of b at the temperature of the first point. In the pure sample, a sharp peak in the derivative occurs at 180.5 K, but the peak is rapidly broadened and shifted in temperature with small W substitution.

Figure 3 shows the resistance versus temperature for nominally pure $K_{0.30}MoO_3$. Metallic behavior is observed from room temperature to 180 K. Below this, the resistance rises steeply and the material becomes semiconducting. The inset shows in detail the behavior near the 180-K transition. A slight rounding in the resistive change near T_0 could be intrinsic, arising from fluctuations, or extrinsic, caused by residual defects or impurities. Figure 4 shows that the resistance data can be fitted to a $\log \rho$ -vs- $1/T$ form below about 67 K. Data could not be obtained below ≈ 30 K because the material becomes highly resistive. The activation energy obtained from Fig. 4 is

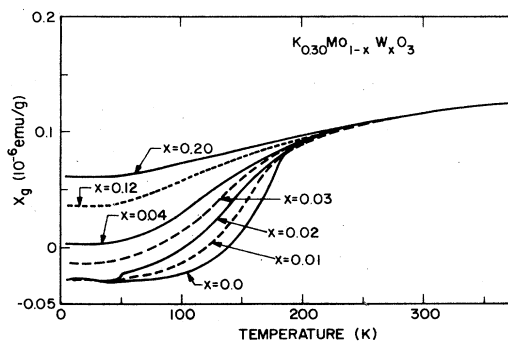


FIG. 1. Susceptibility vs temperature for a series of tungsten-substituted $K_{0.30}MoO_3$ samples.

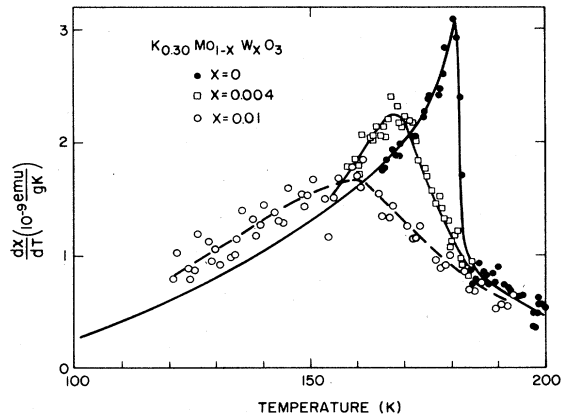


FIG. 2. $d\chi/dT$ vs temperature for $K_{0.30}Mo_{1-x}W_xO_3$ samples.

350 K, leading to a ratio of gap to transition temperature of $2\Delta/T_0 \approx 3.9$. This gap is close to the BCS value obtained from a simple one-dimensional CDW model,²¹ ($2\Delta/T_0 \approx 3.7$), but is much smaller than that obtained for other materials tetrathiafulvalene-tetracyanoquinodimethane (TTF-TCNO), $2\Delta/T_0 \approx 10$ (Ref. 22), $2H-TaSe_2$, $2\Delta/T_0 \approx 25$ (Ref. 23). However, some caution should be exercised in interpreting the resistivity, in this manner, since the data also fits a $\log \rho$ -vs- $1/(T^{0.5})$ form below about 150 K, as shown in Fig. 5. Our inability to measure the resistivity below 30 K precludes us from obtaining data over a sufficiently large resistivity range to differentiate between these two fits to the data.

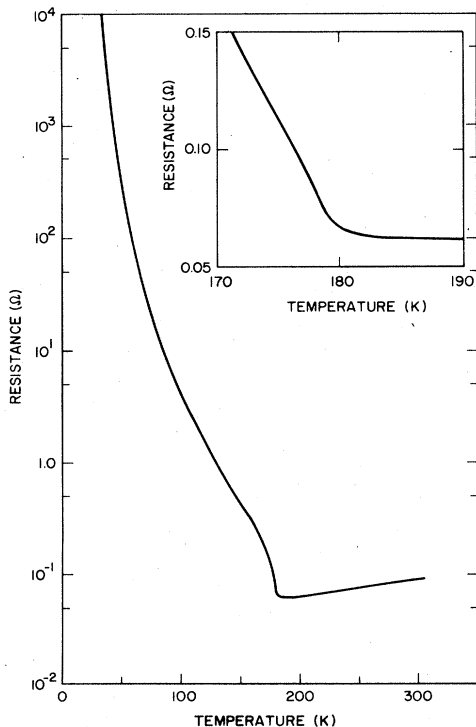


FIG. 3. log resistance vs temperature for $K_{0.30}MoO_3$. Inset shows the region of the phase transition in detail.

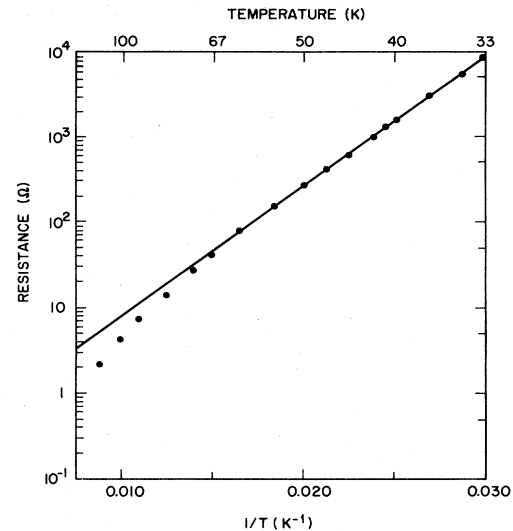


FIG. 4. log resistance vs inverse temperature for $K_{0.30}MoO_3$.

Figure 6 shows the resistivity normalized to the room-temperature value vs temperature for a series of tungsten-substituted $K_{0.30}MoO_3$ samples. Even at very low tungsten-doping levels, a rapid rounding of the break near T_0 is observed. The effects of the doping extend to temperatures well above T_0 . By 3% tungsten, the resistivity no longer shows metallic-type behavior below room temperature, but rather increases with decreasing temperature, with the increase becoming steeper below 180 K. To examine the transition more carefully, a plot of $p^{-1}d\rho/dT$ versus temperature is shown in Fig. 7. Again we can observe the anomaly to shift rapidly to lower temperature and broaden with increasing tungsten concentration.

Susceptibility versus temperature was also measured in a series of rubidium-substituted $K_{0.30}MoO_3$ samples; similar behavior is observed for samples in this series. Differences in the behavior are more easily observed in the numerical derivative (taken as described above) versus temperature as shown in Fig. 8 for $Rb_{0.30}MoO_3$

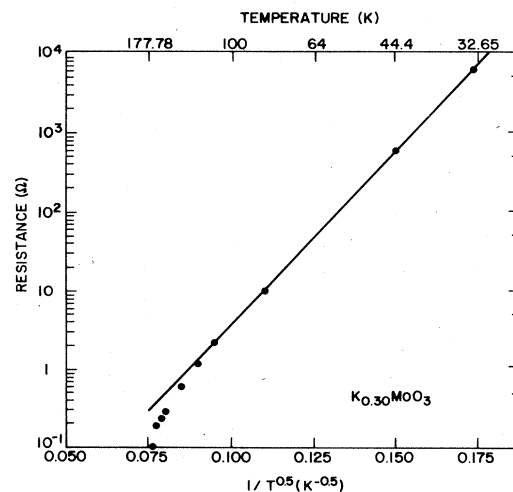


FIG. 5. log resistance vs $1/T^{0.5}$ for $K_{0.30}MoO_3$.

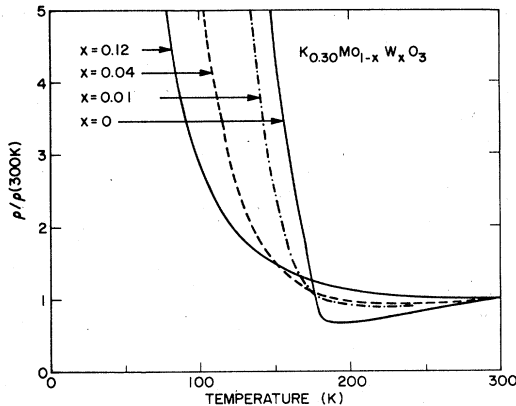


FIG. 6. Resistance normalized to the room-temperature value vs temperature for $K_{0.30}Mo_{1-x}W_xO_3$ samples.

and $K_{0.15}Rb_{0.15}MoO_3$. The derivative data for $K_{0.05}Rb_{0.25}MoO_3$ show a similar broadening resulting from alkali disorder, but the center of the peak is 6.5 K lower than the peak in pure $Rb_{0.30}MoO_3$ (in contrast to the 9.5-K shift seen in Fig. 8). However, as expected, the effects on the susceptibility anomaly caused by alkali substitution are clearly much less dramatic than those due to tungsten substitution.

DISCUSSION

The electrical properties of $K_{0.30}MoO_3$ (or $Rb_{0.30}MoO_3$), which have layered structures consisting of sheets of MoO_3 separated by potassium ions,²⁴ are anisotropic. For example, the resistivity at room temperature is a factor of 10 and 100 times higher along two directions perpendicular to the highly conducting b axis²⁰ [in the $(\bar{2}01)$ plane and perpendicular to these planes, respectively]. Also, the optical reflectivity has been interpreted in terms of quasi-one-dimensional behavior as showing a Drude edge as typical of metals only when the electric field is polarized along the b axis.¹⁶ In the CDW state, the nonlinear properties are observed only along the highly conducting axis,²⁰ again suggesting quasi-one-dimensional behavior. However, the CDW that is ob-

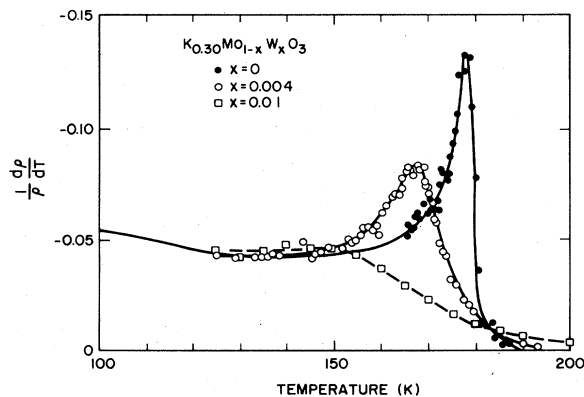


FIG. 7. $\rho^{-1}d\rho/dT$ vs temperature for $K_{0.30}Mo_{1-x}W_xO_3$ samples.

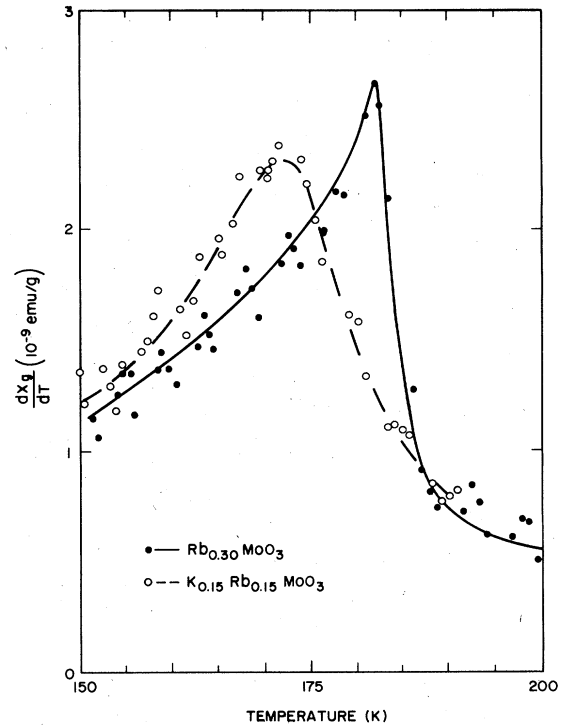


FIG. 8. $d\chi/dT$ vs temperature for $Rb_{0.30}MoO_3$ and $K_{0.15}Rb_{0.15}MoO_3$.

served below 180 K has the full three-dimensional order,²⁵ presumably due to interchain coupling. Above this temperature, strong fluctuations into the CDW state are suggested by the observation of a temperature dependent susceptibility that extends above 300 K. Moreover, rod-shaped x-ray diffuse scattering has been reported above the phase transition, suggesting quasi-two-dimensional correlations.¹

As discussed earlier, the presence of impurities or disorder prevents the establishment of long-range order CDW systems, with the limiting value of the coherence length determined by the strength of the impurity potential and the impurity concentration. Experimentally, the properties of a material with impurities usually show anomalous behavior in the temperature interval where the coherence length is growing rapidly towards its saturation value. If the impurity levels are low enough, a "crossover temperature" can be defined. For example, in nominally pure $K_{0.30}MoO_3$ the derivatives of the magnetic susceptibility or resistivity show rather sharp peaks, which can be used to define this crossover temperature, T_p . However, even in nominally pure $K_{0.30}MoO_3$, the values of T_p obtained from these two properties differ about 2 K (from $d\chi/dT$, $T_p = 180.5$ K and from $\rho^{-1}d\rho/dT$, $T_p = 178.5$ K). At a tungsten-substitution level of only 1% the peaks in the derivative data are essentially lost, making it difficult to define a transition temperature. At $x = 0.004$, however, broadened peaks are reasonably well defined and we can obtain $dT_p/dx \sim 31$ K/mol% W from Fig. 2 or 27 K/mol% W from Fig. 7, which agree within the experimental uncertainty of the derivative data. This value of

dT_p/dx makes it somewhat surprising that nonlinear behavior in the electric properties at 77 K is still observed with 12 mol % W substitution.²⁶ It would appear then that even the short coherence-length distortions about each impurity can lead to some sort of collective effects in the electrical response. It may be that at low temperatures these incoherent distortions freeze into a random configuration analogous to spin glasses²⁷ and that the nonlinear behavior is associated with the dynamics of this distribution of domains.

In contrast to the strong effects of tungsten substitution, the effects of disorder produced by alkali substitution are quite small. Using the derivative of the susceptibility of $K_{0.05}Rb_{0.25}MoO_3$, we find $dT_p/dx = 1.2$ K/mol % alkali substitution, approximately 30 times smaller than the rate of change induced by tungsten substitution.

The decrease in susceptibility of $K_{0.30}MoO_3$ below the CDW onset temperature results from the loss of the Fermi surface by the formation of gaps. Consequently, the Pauli susceptibility due to the carriers is lost. The total susceptibility well below the transition temperature is a sum of core diamagnetic and Van Vleck paramagnetic

contributions. The latter is due to the second-order coupling of the fully occupied d subband formed by the gaps to all of the unoccupied d bands. Part of the Van Vleck contribution, therefore, is inversely proportional to the CDW gap. When impurities are present, a local gap and susceptibility may be defined using the coherence length as a scale. As the impurity level is increased, the distribution of the local gap energies broadens and some states may appear in the gap due to the disorder.^{9,28,29} The increase in the low-temperature susceptibility with increasing tungsten concentration reflects the decreasing average local gap that occurs as the coherence length is diminished (or equivalently, it reflects the decreasing CDW distortions of the lattice with increasing tungsten concentration). The data obtained on the $K_{0.30}Mo_{1-x}W_xO_3$ system suggest that the CDW coherence length becomes very short at low tungsten concentrations.

ACKNOWLEDGMENTS

Useful discussions with P. B. Littlewood, D. S. Fisher, and R. M. Fleming are gratefully acknowledged. The authors thank S. M. Vincent for Fluorescence Microprobe examinations of some samples.

- ¹J. P. Pouget, S. Kagoshima, C. Schlenker, and J. Dumas, *J. Phys. (Paris) Lett.* **44**, L113 (1983).
- ²J. Dumas, C. Schlenker, J. Marcus, and R. Buder, *Phys. Rev. Lett.* **50**, 757 (1983).
- ³For reviews of the nonlinear response of $NbSe_3$ and related compounds, see R. M. Fleming, in *Physics in One Dimension*, Vol. 23 of *Springer Series in Solid State Sciences*, edited by J. Bernasconi and T. Schneider (Springer, New York, 1981), N. P. Ong, *Can. J. Phys.* **60**, 757 (1982), or G. Gruner, *Comments Solid State Phys.* **10**, 183 (1983).
- ⁴Z. Wang, M. C. Saint-Lager, P. Monceau, M. Renard, P. Gressier, A. Meerschaut, L. Guemas, and J. Rouxel, *Solid State Commun.* **46**, 325 (1983).
- ⁵N. P. Ong, J. W. Brill, J. C. Eckert, J. W. Savage, S. K. Khanna, and R. B. Somoano, *Phys. Rev. Lett.* **42**, 811 (1979).
- ⁶J. W. Brill, N. P. Ong, J. C. Eckert, J. W. Sauvage, S. K. Khanna, and R. B. Somoano, *Phys. Rev. B* **23**, 1517 (1981).
- ⁷P. A. Lee and T. M. Rice, *Phys. Rev. B* **19**, 3970 (1979).
- ⁸M. Ido, K. Tsutsumi, T. Sambongi, and N. Mori, *Solid State Commun.* **29**, 399 (1979).
- ⁹R. M. Fleming, D. E. Moncton, and L. F. Schneemeyer (unpublished).
- ¹⁰W. L. McMillan, *Phys. Rev. B* **14**, 1496 (1976).
- ¹¹Y. Imry and S.-k. Ma, *Phys. Rev. Lett.* **35**, 1399 (1975).
- ¹²R. M. Fleming, D. E. Moncton, J. D. Axe, and G. Johnson (unpublished).
- ¹³P. Monceau, J. Richard, and R. Lagnier, *J. Phys. C* **14**, 2995 (1981).
- ¹⁴W. W. Fuller, P. M. Chaikin, and N. P. Ong, *Solid State Commun.* **39**, 547 (1981).
- ¹⁵G. Mihaly, L. Mihaly, and H. Mutka, *Solid State Commun.* **49**, 1009 (1984).
- ¹⁶G. Travaglini, P. Wachter, J. Marcus, and C. Schlenker, *Solid State Commun.* **37**, 599 (1981).
- ¹⁷R. Brusetti, B. K. Chakraverty, J. Devenyi, J. Dumas, J. Marcus, and C. Schlenker, in *Recent Developments in Condensed Matter Physics*, edited by J. T. Devreese *et al.* (Plenum, New York, 1982), Vol. 2.
- ¹⁸A. Wold, W. Kunmann, R. J. Arnott, and A. Ferretti, *Inorg. Chem.* **3**, 545 (1964).
- ¹⁹F. J. DiSalvo and J. V. Waszczak, *Phys. Rev. B* **23**, 457 (1981).
- ²⁰L. F. Schneemeyer, F. J. DiSalvo, J. V. Waszczak, and R. M. Fleming (unpublished).
- ²¹M. J. Rice and S. Strassler, *Solid State Commun.* **13**, 125 (1973).
- ²²S. Etemad, *Phys. Rev. B* **13**, 2254 (1976).
- ²³W. L. McMillan, *Phys. Rev. B* **16**, 643 (1977).
- ²⁴J. Graham and A. D. Wadsley, *Acta Crystallogr.* **20**, 93 (1966).
- ²⁵P. A. Lee, T. M. Rice, and P. W. Anderson, *Solid State Commun.* **14**, 703 (1974).
- ²⁶L. F. Schneemeyer, R. M. Fleming, and S. E. Spengler (unpublished).
- ²⁷R. M. Fleming and L. F. Schneemeyer, *Phys. Rev. B* **28**, 6996 (1983).
- ²⁸W. L. McMillan, *Phys. Rev. B* **12**, 1187 (1975).
- ²⁹H. Fukuyama, *J. Phys. Soc. Jpn.* **41**, 513 (1976).